ELSEVIER

Journal of Molecular Catalysis A: Chemical 147 (1999) 179–190

JOURNAL OF MOLECULAR CATALYSIS A: CHEMICAL

www.elsevier.com/locate/molcata

Photochemical self-assembly reactions of polyoxovanadates [1] Structure of MoO_4^{2-}-encapsulated mixed-valent cluster $[V_{22}O_{54}(MoO_4)]^{8-}$ and template-exchange reaction of $[V_{18}O_{42}(H_2O)]^{12-}$

Toshihiro Yamase *, Lan Yang, Riéko Suzuki

Research Laboratory of Resources Utilization, Tokyo Institute of Technology, 4259 Nagatsuta, Midori-ku, Yokohama 226-8503, Japan

Abstract

Prolonged photolysis of aqueous solution containing $[V_4O_{12}]^{4-}$ and MeOH at pH 5.5 in the presence of K_2MoO_4 leads to the formation of $K_6H_2[V_{22}O_{54}(MoO_4)] \cdot 19H_2O$ (**1**). The anion of **1**, formally written as $[V_8^{IV}V_{14}^{V}O_{54}(MoO_4)]^{8-}$, forms cluster shell with approximate D_{2d} symmetry as a subgroup of T_d symmetry for MoO_4^{2-}. The interaction of the oblong and egg-shaped $\{V_{22}O_{54}\}$ cluster shell encapsulated by MoO_4^{2-} is stronger than that of the ClO_4^--encapsulated anion with the same topology but there is still no significant bonding of the shell V atoms to the template O atoms (with V · · · O(Mo) distances of > 2.7 Å). The template-exchange reaction of $[V_{18}^{IV}O_{42}(H_2O)]^{12-}$ with small anions occurs via oxidative splitting of V^{IV}–O–V^{IV} bond of the shell cluster to yield the mixed-valent polyoxovanadate clusters, the structure of which reflects symmetry, charge, and disorder of the central anion template.

Keywords: MoO_4^{2-}-encapsulated polyoxovanadate; Photoencapsulation; Template-exchange reaction; X-ray diffractometry; Self-assembly reaction

1. Introduction

$[HV_2O_7]^{3-}$, which is in equilibrium with $[V_4O_{12}]^{4-}$ in basic media, is photosensitive and works as a photocatalyst for the H_2 formation from electron-donative organic substances [1]. These vanadate species undergo the photochemical self-assembly reaction in the presence of small charged or neutral species as templates to yield the spherical polyoxovanadate cluster encapsulated by the small species [2–5]. The chemically induced dynamic electron polarization (CIDEP) spectroscopy of the polyoxometalate/alcohol systems reveals that the reaction precursor involved in the photoredox reaction of the polyoxometalates is the $O \rightarrow M$ LMCT triplet states which abstracts a hydrogen from alcohols (electron donor) to yield a singly protonated polyoxometalate and α-hydroxyalkyl radicals [2]. The shape of the cluster anion (with a central cavity-size of 5–10 Å diameter) strongly depends on the symmetry of the template. Most of the clusters consist of pentagonal OVO_4 pyramids, and additional VO_6 octahedra are configurated as shown for $[V_{15}O_{36}(CO_3)]^{7-}$ and

* Corresponding author

[1] Photochemistry of polyoxovanadates. Part 4.

1381-1169/99/$ - see front matter
PII: S1381-1169(99)00142-9

$[V_{18}O_{42}(PO_4)]^{11-}$. Fig. 1 exemplifies structures of these spherical anion clusters: mixed-valence anions, $[V_{15}O_{36}(CO_3)]^{7-}$, $[V_{18}O_{42}(Cl)]^{13-}$, $[V_{18}O_{44}(N_3)]^{14-}$, and $[V_{12}B_{32}O_{76}(OH)_8(Na_4)]^{7-}$ indicate approximate symmetries of D_{3h}, D_{4d}, D_{2h}, and D_{4h}, respectively. Four sodium cations in the latter are disordered on eight positions of central tetragonal corners. Alkaline-metal cation-encapsulated clusters also have been characterized for the polyoxotungstates $[Sb_9W_{21}O_{86}(Na)]^{18-}$ [6], $[As_4W_{40}O_{140}(K)]^{8-}$ [7], $[W_{18}O_{56}(HF_3)_2(Na)]^{7-}$ [8], and $[P_5W_{30}O_{110}(Na)]^{14-}$ [9]. Another type of oxovanadium/borate cluster $(enH_2)_5[V_{12}B_{18}O_{54}(OH)_6] \cdot H_2O$ (en = ethylenediamine), in which the anion consists of a puckered $B_{18}O_{36}(OH)_6$ ring sandwiched between two triangles of six edge-shared vanadium atoms without any feasibility of encapsulation, can be hydrothermally synthesized at 170°C in water [10]. In addition, the $[V_{12}B_{32}O_{76}(OH)_8]$ cluster has recently been isolated in the compound $(H_3O)_{12}[V_{12}B_{32}O_{76}(OH)_8] \cdot 28H_2O$ under the hydrothermal reaction at 170°C [11].

The photochemical encapsulation allows the preparation processes to be easily controlled and provides many opportunities to prepare mixed-valence isomers of the spherical polyoxovanadates obtained by Pope and Müller [12] and Müller et al. [13,14]. In our continuous work on the photoencapsulation of polyoxovanadates, we describe here the photoencapsulation in the presence of molybdates which leads to the formation of $K_6H_2[V_{22}O_{54}(MoO_4)] \cdot 19H_2O$ (**1**). The $\{V_{22}O_{54}\}$ cluster shell of the $[V^{IV}{}_8V^{V}{}_{14}O_{54}(MoO_4)]^{8-}$ anion of **1** is the same as for $[HV^{IV}{}_8V^{V}{}_{14}O_{54}(ClO_4)]^{6-}$ [15], $[HV^{IV}{}_8V^{V}{}_{14}O_{54}(SCN)]^{6-}$ [16], and $[H_2V^{IV}{}_{10}V^{V}{}_{12}O_{54}(CH_3CO_2)]^{7-}$ [16]. There is no report of the structure of the MoO_4^{2-}-encapsulated spherical polyoxovanadate, although the $\{V_{22}O_{54}\}$ shell is expected on the encapsulation of MoO_4^{2-} [14]. In addition, we describe the template-exchange reaction of $[V^{IV}{}_{18}O_{42}(H_2O)]^{12-}$ with CO_3^{2-},N_3^-, SCN^- and NO_3^-, which influence the shell built up around the templates. The $[V^{IV}{}_{18}O_{42}(H_2O)]^{12-}$ anion contains H_2O in the central cavity with long distances (V · · · $O(H_2)$, 3.80 and O · · · $O(H_2)$, 3.57 Å in average) between the oxygen atom of H_2O and the shell (linked by 18 tetragonal OVO_4 pyramids) atoms of electrophilic 18 V and nucleophilic 24O sites, indicating a pseudomechanical fixing of the H_2O (hostage) (Fig. 1B) [3,12]. Such high coordination numbers (42) of H_2O molecule seems to allow the H_2O molecule to be exchanged by the outside template. The laws governing the template-exchange processes are still unknown and the control of the topological linkage of this type of clusters is also important in the poorly understood mechanism of ion exchange through membranes which occurs very rapidly. The present work will be useful not only for a synthetic study of the high-nuclearity oxovanadate complexes but also in a model of the ion-exchange through membrane.

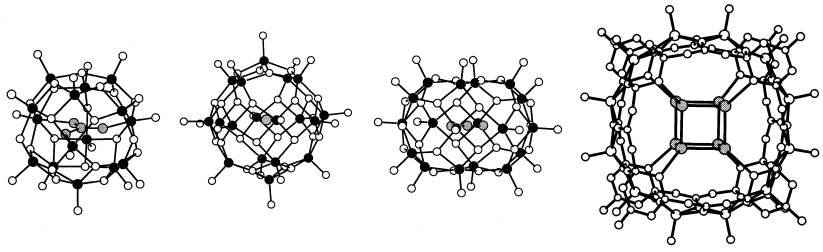

Fig. 1. Structures of spherical cluster anions produced by photoinduced self-assembly encapsulation: (A) $[V_{15}O_{36}(CO_3)]^{7-}$, (B) $[V_{18}O_{42}(Cl)]^{13-}$, (C) $[V_{18}O_{44}(N_3)]^{14-}$, and (D) $[V_{12}B_{32}O_{76}(OH)_8(Na_4)]^{7-}$.

2. Experimental

2.1. Photoencapsulation procedure

All the reagents were of at least analytical grade and used without further purification. The salt $[NH_3Bu^t]_4[V_4O_{12}]$ was synthesized according to the published procedure and identified in the solid state by comparison of the IR spectrum with that previously reported [17]. $K_6H_2[V_{22}O_{54}(MoO_4)] \cdot 19H_2O$ (**1**) was prepared as follows: an aqueous solution containing $[NH_3Bu^t]_4[V_4O_{12}]$ (0.8 g, 1.2 mmol) and $K_2MoO_4 \cdot 2H_2O$ (0.6 g, 2.5 mmol) in water (60 cm^3) in a Pyrex tube (20 cm^3) was adjusted to pH 5.5 with 12 N-HCl and MeOH (6 cm^3) was added. The resulting solution was irradiated for 5 days under an atmosphere of nitrogen using a 500 W superhigh-pressure mercury lamp. Black single plate-like crystals were precipitated within 2–3 days at 5°C in the photolyte after irradiation with a yield of 0.34 g.

The vanadium content of **1** was determined using the potentiometric method by detecting the end-points of titrations with Fe^{2+} (for V^V) and Mn^{7+} (for V^{IV}) in stirred H_2SO_4 solutions. Measurements of the potential using a Pt indicator electrode vs. Ag–AgCl reference electrode at open circuit were carried out using a TOA Electronics IM-5S ion meter: a known excess of ammonium iron(II) sulfate was added to the sample in 1 mol dm^{-3} H_2SO_4 to reduce V^V to V^{IV} which was determined using a standard solution of $KMnO_4$. The potentiometric back titration of **1** gave eight(8 ± 0.2)-electron reduction per anion, which correspond to the numbers of V^{IV} centers in the anions. IR spectra were recorded on JASCO FT/IR-5000 spectrometer.

2.2. Template-exchange reaction procedure

$Na_{12}[V_{18}O_{42}(H_2O)] \cdot 23H_2O$ was prepared according to Ref. [18] and characterized by elemental analysis, IR spectrum, and potentiometric titration analysis (for V^{IV}). Small

Table 1
Crystal and refinement data for $K_6H_2[V_{22}O_{54}(MoO_4)] \cdot 19H_2O$ (**1**)

Formula	$H_{40}O_{77}K_6V_{22}Mo$
M	2723.51
Crystal symmetry	Orthorhombic
Space group (number)	*Pnma* (62)
a (Å)	22.90(3)
b (Å)	17.72(2)
c (Å)	20.43(3)
U (Å^3)	8289(15)
Z	4
D_c (g cm^{-3})	2.182
μ (cm^{-1})	29.06
F(000)	5272
Crystal size (mm)	$0.5 \times 0.5 \times 0.3$, orthogonal plate
Data collection range (°)	$2 \leq 2\theta \leq 55$
h,k,l Ranges	0–29, 0–33, 0–25
Number of reflections collected	13081
Number of reflections used in refinement with $[\|F\| > 3\sigma(F)]$	2264
Number of parameters refined	293
Final R	0.104
Final R'	0.080
Goodness of fit, S	3.08
Maximum shift (error)	0.210

Table 2
Atomic coordinates for $K_6H_2[V_{22}O_{54}(MoO_4)] \cdot 19H_2O$ (**1**) with estimated standard deviations (e.s.d.s) in parentheses

Atom	*x*	*y*	*z*	*B*(eq)
Mo(1)	0.2547(2)	0.25	0.0551(3)	3.1(2)
V(1)	0.3520(3)	0.1519(4)	0.2180(3)	2.4(2)
V(2)	0.1908(3)	0.1540(4)	0.2209(3)	2.1(2)
V(3)	0.0733(4)	0.25	0.1490(5)	2.2(3)
V(4)	0.0591(4)	0.25	0.0029(5)	1.9(2)
V(5)	0.1155(3)	0.1002(4)	0.1075(3)	2.3(2)
V(6)	0.1322(5)	0.25	−0.1219(5)	2.9(3)
V(7)	0.1520(3)	0.0984(4)	−0.0583(3)	3.0(2)
V(8)	0.2662(3)	0.1558(4)	−0.1198(3)	2.3(2)
V(9)	0.3025(3)	0.0493(4)	−0.0160(3)	2.4(2)
V(10)	0.4072(3)	0.1526(4)	−0.0372(3)	3.2(2)
V(11)	0.4110(3)	0.0896(4)	0.0989(3)	2.6(2)
V(12)	0.2669(3)	0.0481(4)	0.1449(3)	2.3(2)
V(13)	0.4544(4)	0.25	0.1115(5)	2.4(3)
K(1)	0.2752(4)	0.0398(6)	0.3372(5)	4.5(2)
K(2)	0.4605(7)	0.487(1)	−0.6839(8)	13.6(6)
K(3)	0.099(2)	0.383(3)	−0.607(2)	20(2)
K(4)	0.587(1)	0.031(1)	0.139(1)	6.2(6)
O(1)	0.372(1)	0.112(1)	0.285(1)	1.8(5)
O(2)	0.177(1)	0.110(2)	0.284(1)	3.9(7)
O(3)	0.015(2)	0.25	0.186(2)	7(1)
O(4)	−0.006(2)	0.25	−0.011(2)	4(1)
O(5)	0.078(1)	0.031(1)	0.131(1)	3.5(6)
O(6)	0.090(2)	0.25	−0.181(2)	4(1)
O(7)	0.126(1)	0.030(1)	−0.101(1)	4.0(7)
O(8)	0.278(1)	0.106(1)	−0.183(1)	3.3(6)
O(9)	0.312(1)	−0.021(1)	−0.058(1)	2.9(6)
O(10)	0.457(1)	0.108(2)	−0.083(1)	4.4(7)
O(11)	0.464(1)	0.037(1)	0.112(1)	3.0(6)
O(12)	0.261(1)	−0.025(1)	0.189(1)	2.7(6)
O(13)	0.522(2)	0.25	0.130(2)	2.9(9)
O(14)	0.137(1)	0.075(1)	0.026(1)	2.7(6)
O(15)	0.069(1)	0.182(1)	0.077(1)	3.2(6)
O(16)	0.114(1)	0.175(1)	0.186(1)	2.7(6)
O(17)	0.098(1)	0.180(1)	−0.057(1)	3.3(6)
O(18)	0.198(2)	0.25	0.248(2)	4(1)
O(19)	0.182(1)	0.174(1)	−0.135(1)	2.9(6)
O(20)	0.286(2)	0.25	−0.146(2)	3.0(9)
O(21)	0.275(1)	0.131(1)	0.212(1)	3.3(6)
O(22)	0.235(1)	0.089(1)	−0.056(1)	3.2(6)
O(23)	0.190(1)	0.085(1)	0.145(1)	2.4(6)
O(24)	0.274(1)	0.018(1)	0.061(1)	3.9(6)
O(25)	0.354(1)	0.061(1)	0.153(1)	3.2(6)
O(26)	0.378(1)	0.059(1)	0.024(1)	2.1(5)
O(27)	0.418(1)	0.173(1)	0.164(1)	2.8(6)
O(28)	0.332(1)	0.132(1)	−0.065(1)	2.0(5)
O(29)	0.345(2)	0.25	0.239(2)	3(1)
O(30)	0.408(2)	0.25	−0.064(2)	4(1)
O(31)	0.443(1)	0.170(1)	0.046(1)	2.7(6)
O(32)	0.236(2)	0.25	−0.021(2)	9(1)
O(33)	0.194(2)	0.25	0.100(2)	7(1)
O(34)	0.295(1)	0.169(2)	0.068(2)	8(1)
O(35)	−0.009(2)	0.372(2)	−0.134(2)	12(1)
O(36)	0.202(3)	−0.148(4)	−0.071(3)	27(3)
O(37)	0.139(2)	0.426(2)	−0.241(2)	13(1)

Table 2 (continued)

Atom	*x*	*y*	*z*	*B*(eq)
O(38)	0.361(1)	0.066(1)	−0.280(1)	4.6(7)
O(39)	0.535(3)	0.093(4)	−0.223(4)	30(3)
O(40)	−0.049(1)	0.117(2)	0.093(1)	5.7(8)
O(41)	0.476(1)	−0.107(1)	−0.231(1)	3.4(6)
O(42)	0.443(1)	−0.078(2)	−0.004(2)	9(1)
O(43)	−0.112(1)	0.25	0.129(2)	1.9(8)
O(44)	0.409(3)	0.076(4)	0.511(4)	28(3)

amounts of $NaHCO_3$, NaN_3, and NaSCN solids were added slowly to a solution of freshly prepared $Na_{12}[V_{18}O_{42}(H_2O)] \cdot 23H_2O$ (1 g) in water (50 ml) with further addtion of water, and finally, 5, 10, and 25 g of $NaHCO_3$, NaN_3, and NaSCN were added into a resultant solution (500 ml), respectively. Black crystals of $Na_6H_4[V_{15}O_{36}(CO_3)] \cdot 32H_2O$ (**2**), $Na_{10}H[V_{18}O_{44}(N_3)] \cdot 30H_2O$ (**3**), and $Na_{10}H_2[V_{18}O_{44}(SCN)] \cdot 30H_2O$ (**4**) suitable for single-crystal X-ray diffraction were formed within 2 weeks, 1 month, and 2 months with yields of 0.76, 0.36, and 0.25 g, respectively. Found: C, 0.64; Calc. for $Na_6H_4[V_{15}O_{36}(CO_3)] \cdot 32H_2O$: C, 0.57%. Found: N, 1.75; Calc. for $Na_{10}H[V_{18}O_{44}(N_3)] \cdot 30H_2O$: N, 1.72%. Found: S, 1.41; C, 0.68; N, 0.58; Calc. for $Na_{10}H_2[V_{18}O_{44}(SCN)] \cdot 30H_2O$: S, 1.31; C,0.49; N, 0.57%. Black crystals of $Na_6H_3[V_{18}O_{42}(NO_3)] \cdot 27H_2O$ (**5**) were prepared by a similar procedure (6 g of $Na_{12}[V_{18}O_{42}(H_2O)] \cdot 23H_2O$ and 30 g of $NaNO_3$ for the final solution of 500 ml) with a yield of 2.8 g. Found: N, 0.55; Calc. for $Na_6H_3[V_{18}O_{42}(NO_3)] \cdot 27H_2O$: N, 0.62%.

Cyclic voltammograms were measured with a potentiostat/galvanostat (Hokuto Denko HA-301) and a function generatior (Nikko Keisoku NFG-3). The sample solution containing 5 mM $[Na_{12}[V_{18}O_{42}(H_2O)] \cdot 23H_2O$ (0.8 mM for **2**–**5**) and 50 mM NaOH(0.1 M NaCl for **2**–**5**) in water were purged with argon and measured using a carbon-fiber (33 μm diameter) working electrode, a platinum-wire counter electrode, and a SCE reference electrode. After each measurement the working electrode was polished with 0.3-μm Al_2O_3 (Buehler) and rinsed with water to ensure reproducible results. All electric potentials quoted are with reference to SCE electrode.

The evacuation for the deaeration of sample solutions was carried by several freeze-pump-thaw cycles to 10^{-4} Torr.

2.3. X-ray structural analysis

Crystals were sealed in Lindemann glass capillaries and mounted on a Rigaku AFC-5S diffractometer equipped with graphite crystal monochromatized Mo–K_α ($\lambda = 0.71069$ Å) radiation. The intensities were collected by ω-2θ scans at the 2θ scan rate of 8° min^{-1} at room temperature. The orientation matrix and cell dimensions was obtained from the setting angles of 25 centered reflections in the range $2\theta =$ 20.0–25.0°, for **1**. No significant decay of intensity of the three standard reflections recorded after every 100 reflections was observed. V and Mo positions for **1** were determined by direct methods using MITHRIL 90 [16]. K and O atoms were located from difference syntheses. Lorentz and polarization factors were applied and an absorption correction was made on the basis of Ψ-scans of three reflections [19] after isotropic refinement. The correction factors applicable to $|F_o|$ were 0.93–1.00. Subsequently the Mo and V atoms were refined with anisotropically thermal parameters. Refinements for all non-H atoms were carried out using the full-matrix least-squares method. The quantity minimized was $\sum w(|F_o| - |F_c|)^2$. Attempts to refine potassium and crystal-water oxygen atoms, with various combinations of site occu-

pancy factors were done. A summary of crystal data for **1** is shown in Table 1. The weighting scheme employed was $w^{-1} = \sigma^2(F_o)$, where $\sigma^2(I_o) = \sigma^2(I_{counting}) + (0.006\ I_o)^2$ for **1**. The maximum and minimum heights in the final difference synthesis were 1.5 and -1.1 eÅ^{-3} around K(2) atom at distances of 1.6 and 1.1 Å (with its symmetry equivalent, $-1/2 + x$, $1/2 - y$, $3/2 - z$), respectively. All calculations were carried out on a Micro VAX II computer using the TEXSAN software package [20]. Final atomic coordinates and isotropic thermal parameters are given in Table 2. The bond-strength (s) in valence units was calculated using $s = ((d/1.791)^{-5.1}$, and $(d/1.770)^{-5.2}$ for the V^V–O and V^{IV}–O bond length (d) in Å, respectively [21], and the valence sum (bond order = $\sum s$) of all of the V^V–O and V^{IV}–O bond strengths about a given O atom was estimated for the valence of the atom. Crystal data for **2**–**5** were described elsewhere [22].

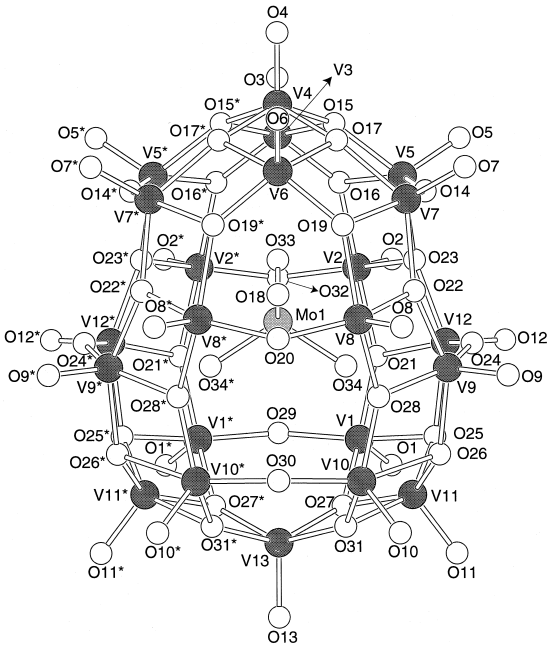

Fig. 3. Schematic representation of the structure of $[V_{12}O_{54}(MoO_4)]^{8-}$ with atom labelling. Asterisked atoms are related to corresponding unasterisked ones by a symmetry equivalent (x, $1/2 - y$, z).

3. Results and discussion

3.1. Structure of $K_6H_2[V_{22}O_{54}(MoO_4)]\cdot 19H_2O$ (1)

The IR spectrum of **1** in KBr is shown in Fig. 2. Strong broad band at 967 cm^{-1} is due to terminal V–O stretching of the cluster formed by linking VO_5 polyhedra and the feature at 700–600 cm^{-1} is attributed to symmetric and asymmetric V–O–V stretchings. The strong bands at 812 cm^{-1} can be assigned to $\nu_{asym(Mo-O)}$ stretching mode.

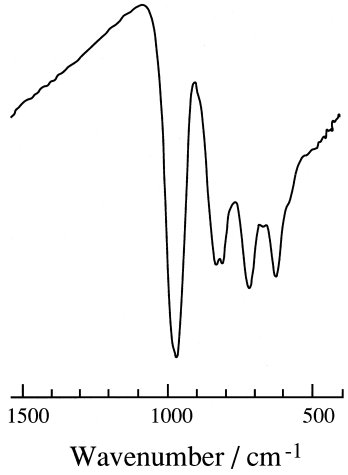

Fig. 2. IR spectrum of $K_6H_2[V_{12}O_{54}(MoO_4)]\cdot 19H_2O$ (**1**).

The unit cells for **1** contains four molecules. Fig. 3 shows a view of anion structure of **1**. The anion has approximate D_{2d} symmetry (42 m). Chemical and X-ray structural analyses of **1** formally reveal the presence of six K^+ cations for each molecule. All of the K atoms have five to seven contacts to the anion and water O atoms with K···O distances of 2.41(6)–3.07(5) Å. Two K atoms (K(3) and K(4)) are disordered with their symmetry equivalent ($-1/2 + x$, $1/2 - y$, $3/2 - z$) in the short distance 1.67(5) Å and refined with half occupancies. Nineteen O atoms of water molecules of crystallization were located and some of them had large temperature factors due to disorder-

ing. In conjunction with the potentiometric titration result which indicated the eight-electron reduction per anion, thus, **1** indicates the composition of $K_6H_2[V^{IV}_{8}V^{V}_{14}O_{54}(MoO_4)] \cdot 19H_2O$, to maintain electrical neutrality. The same structure of the shell has been reported for $[NEt_4]_6[HV_{22}O_{54}(ClO_4)]$, $[NEt_4]_6[HV_{22}O_{54}(SCN)]$, and $[NEt_4]_5(NH_4)_2[H_2V_{22}O_{54}(CH_3CO_2)] \cdot 7H_2O$, which were prepared by the reaction of $[NH_4]_8[H_9V_{19}O_{50}] \cdot 11H_2O$ and NEt_4^+ salts of corresponding template anions in water for 60 h at 75°C [15,16]. The $[V_{22}O_{54}(MoO_4)]^{8-}$ anion indicates the oblong and egg-shaped $\{V_{22}O_{54}\}$ cluster shell encapsulating negatively charged MoO_4^{2-}, which is built up of edge-and corner-sharing OVO_4 square pyramids at neighboring V · · · V distances of 2.948(9)–3.08(1) Å [mean, 3.02(1) Å for 24 bonds] and 3.34(1)–3.691(9) Å [mean, 3.56(2) Å for 32 bonds], respectively. Table 3 shows selected bond distances and bond angles. V=O, V–O(μ_2), and V–O(μ_3) bond distances are 1.52(4)–1.67(3) [mean, 1.58(2)], 1.79(3)–1.81(3) [mean, 1.80(3)], and 1.78(2)–2.18(2) [mean, 1.93(3)] Å, respectively. A simplified vanadium-atom framework of **1** is shown in Fig. 4 where asterisked atoms indicate the symmetry equivalent $(x, 1/2-y, z)$ atoms. The framework consists of two sets of four horizontal rectangle planes V(5,5*,7*,7), V(2,2*,8*,8), V(12,12*,9*,9), and V(1,1*,10*,10), and a set of two vertical polar triangle planes V(4,3,6) and V(13,11*,11). The two sets of the rectangle planes with average sizes of $5.35(2) \times 3.49(1)$ Å and $7.16(1) \times 3.40(1)$ Å in V · · · V distances are orientated perpendicular to the S_4 axis through polar V(4) and V(13) atoms which is related by vertical mirror planes V(4,3,13,6) and V(4,11,13,11*), as shown in Fig. 3. The polar triangle plane was in an average size of 3.02(1), 3.02(1), and 5.69(1) Å in V · · · V distances. The polar vanadium atoms V(4) and V(13) were at distance of 9.32(2) Å. Such a feature of the anion for **1** is similar to that (9.40 Å in polar V · · · V distance, and 6.00 and 7.00 Å in V · · · V widths) for $[V_{22}O_{54}(ClO_4)]^{7-}$ [15]. The central MoO_4 tetrahedral environment indicates the O–Mo–O angles ranging from 107(1)–113(2)° and the mean Mo–O bond distance of 1.68(1) Å. Although the O · · · O (mean 2.75(5) Å in 2.66(6)–2.87(6) Å) and Mo–O (mean 1.68(4) Å in 1.62(5)–1.72(3) Å) distances in the tetrahedral MoO_4^{2-} ion are longer than the corresponding O · · · O (2.29–2.37 Å) and Cl–O (1.41–1.48 Å) distances in the ClO_4^- ion of $[V_{22}O_{54}(ClO_4)]^{7-}$, in both cases topologically equivalent shells are formed. As for the interaction between the MoO_4^{2-} ion and the cluster shell, the shortest O(Mo) · · · V distances 2.70(4)–3.00(4) Å [mean, 2.80(4) Å] for **1** are shorter than the comparable O(Cl) · · · V distances (> 2.96 Å) between the central ClO_4^- anion and the cluster shell for $[V_{22}O_{54}(ClO_4)]^{7-}$ [15]. Therefore, it is noteworthy that the $MoO_4^{2-} \leftrightarrow$ shell interaction is stronger than that of the ClO_4^--encapsulated species, due to an electrostatic interaction with a more negatively charged MoO_4^{2-} ion compared to ClO_4^-. However, it is possible to say that the four terminal O atoms bound to the Mo atom within cluster shell do not show any significant bonding to the V atoms of the shell, since the O(Mo) · · · V distances (> 2.7 Å) would otherwise be less than 2.4 Å with a resultant longer Mo–O bonds. The point group (D_{2d}) of the cluster shell of **1** with highly symmetric template (T_d symmetry) corresponds to a subgroup of the point group of the latter. This let us to confirm the conclusion that the symmetry of the cluster shell of the spherical polyoxovanadates strongly reflects by that of the encapsulated template [5,12].

The hydrogen atoms could not be located directly from the three-dimensional X-ray diffraction data. The result of bond-valence sum calculations indicates no plausible coordination of H^+ on the shell oxygen atoms, although two V=O terminal O atoms, O(7) and O(10) gave the valence sum of 1.4–1.6. In addition, based on the bond-valence sum calculations, the V^{IV} center in the anion was presumed to be disordered over all of the OVO_4 sites.

Table 3
Selected bond distances (Å) and angles (°) for $K_6H_2[V_{22}O_{54}(MoO_4)] \cdot 19H_2O$ (**1**)

Mo(1)–O(32)	1.62(5)	V(1)–O(1)	1.61(2)	V(2)–O(2)	1.54(3)
Mo(1)–O(33)	1.67(4)	V(1)–O(21)	1.81(3)	V(2)–O(16)	1.94(2)
Mo(1)–O(34)	1.72(3)	V(1)–O(25)	2.08(3)	V(2)–O(18)	1.79(1)
Mo(1)–O(34^{VII})	1.72(3)	V(1)–O(27)	1.90(2)	V(2)–O(21)	1.98(3)
		V(1)–O(29)	1.80(1)	V(2)–O(23)	1.97(2)
V(3)–O(3)	1.53(5)	V(4)–O(4)	1.52(4)	V(5)–O(5)	1.58(3)
V(3)–O(15)	1.91(2)	V(4)–O(15)	1.94(2)	V(5)–O(14)	1.80(2)
V(3)–O(15^{VII})	1.91(2)	V(4)–O(15^{VII})	1.94(2)	V(5)–O(15)	1.91(2)
V(3)–O(16)	1.78(2)	V(4)–O(17)	1.95(2)	V(5)–O(16)	2.08(2)
V(3)–O(16^{VII})	1.78(2)	V(4)–O(17^{VII})	1.95(2)	V(5)–O(23)	1.89(2)
V(6)–O(6)	1.55(4)	V(7)–O(7)	1.60(3)	V(8)–O(8)	1.58(2)
V(6)–O(17)	1.98(2)	V(7)–O(14)	1.80(2)	V(8)–O(19)	1.98(2)
V(6)–O(17^{VII})	1.98(2)	V(7)–O(17)	1.91(2)	V(8)–O(20)	1.81(1)
V(6)–O(19)	1.78(2)	V(7)–O(19)	2.17(2)	V(8)–O(22)	1.89(2)
V(6)–O(19^{VII})	1.78(2)	V(7)–O(22)	1.92(3)	V(8)–O(28)	1.92(2)
				V(8)–O(32)	2.70(4)
V(9)–O(9)	1.53(2)	V(10)–O(10)	1.67(3)	V(11)–O(11)	1.56(2)
V(9)–O(22)	1.88(2)	V(10)–O(26)	2.18(2)	V(11)–O(25)	1.79(3)
V(9)–O(24)	1.79(3)	V(10)–O(28)	1.85(2)	V(11)–O(26)	1.79(2)
V(9)–O(26)	1.93(2)	V(10)–O(30)	1.81(1)	V(11)–O(27)	1.98(2)
V(9)–O(28)	1.90(2)	V(10)–O(31)	1.92(2)	V(11)–O(31)	1.94(2)
V(9)–O(34)	2.73(3)				
V(12)–O(12)	1.58(2)	V(13)–O(13)	1.60(3)	O(32)–O(33)	2.66(6)
V(12)–O(21)	2.01(2)	V(13)–O(27)	1.93(2)	O(32)–O(34)	2.68(5)
V(12)–O(23)	1.88(2)	V(13)–O(27^{VII})	1.93(2)	O(32)–O(34^{VII})	2.68(5)
V(12)–O(24)	1.81(3)	V(13)–O(31)	1.95(2)	O(33)–O(34)	2.80(4)
V(12)–O(25)	2.01(3)	V(13)–O(31^{VII})	1.95(2)	O(33)–O(34^{VII})	2.80(4)
V(12)–O(34)	2.74(3)			O(34)–O(34^{VII})	2.87(6)
O(32)–Mo(1)–O(33)	108(2)	O(1)–V(1)–O(21)	104(1)	O(2)–V(2)–O(16)	103(1)
O(32)–Mo(1)–O(34)	107(1)	O(1)–V(1)–O(25)	101(1)	O(2)–V(2)–O(18)	104(2)
O(33)–Mo(1)–O(34)	111(1)	O(1)–V(1)–O(27)	111(1)	O(2)–V(2)–O(21)	99(1)
O(34)–Mo(1)–O(34^{VII})	113(2)	O(1)–V(1)–O(29)	104(1)	O(2)–V(2)–O(23)	110(1)
		O(21)–V(1)–O(25)	79(1)	O(16)–V(2)–O(18)	91(1)
		O(21)–V(1)–O(27)	140(1)	O(16)–V(2)–O(21)	153(1)
		O(21)–V(1)–O(29)	97(1)	O(16)–V(2)–O(23)	80(1)
		O(25)–V(1)–O(27)	76(1)	O(18)–V(2)–O(21)	98(1)
		O(25)–V(1)–O(29)	154(1)	O(18)–V(2)–O(23)	146(1)
		O(27)–V(1)–O(29)	92(1)	O(21)–V(2)–O(23)	78.7(9)
O(3)–V(3)–O(15)	110(1)	O(4)–V(4)–O(15)	105(1)	O(5)–V(5)–O(14)	104(1)
O(3)–V(3)–O(16)	104(1)	O(4)–V(4)–O(17)	110(1)	O(5)–V(5)–O(15)	113(1)
O(15)–V(3)–O(15^{VII})	78(1)	O(15)–V(4)–O(15^{VII})	76(1)	O(5)–V(5)–O(16)	104(1)
O(15)–V(3)–O(16)	84(1)	O(15)–V(4)–O(17)	92(1)	O(14)–V(5)–O(15)	92(1)
O(15)–V(3)–O(16^{VII})	145(1)	O(15)–V(4)–O(17^{VII})	145(1)	O(14)–V(5)–O(16)	152(1)
O(16)–V(3)–O(16^{VII})	96(2)	O(17)–V(4)–O(17^{VII})	79(1)	O(14)–V(5)–O(23)	96(1)
				O(15)–V(5)–O(16)	76(1)
				O(15)–V(5)–O(23)	138(1)
				O(16)–V(5)–O(23)	78(1)
O(11)–V(11)–O(25)	107(1)	O(13)–V(13)–O(27)	107(1)		
O(11)–V(11)–O(26)	107(1)	O(13)–V(13)–O(31)	107(1)		
O(11)–V(11)–O(27)	106(1)	O(27)–V(13)–O(27^{VII})	90(1)		
O(11)–V(11)–O(31)	104(1)	O(27)–V(13)–O(31)	78.8(9)		
O(25)–V(11)–O(26)	98(1)	O(27)–V(13)–O(31^{VII})	146(1)		
O(25)–V(11)–O(27)	81(1)	O(31)–V(13)–O(31^{VII})	92(1)		
O(25)–V(11)–O(31)	146(1)				

Table 3 (continued)

O(26)–V(11)–O(27)	146(1)
O(26)–V(11)–O(31)	85(1)
O(27)–V(11)–O(31)	78(1)

Symmetry codes: VII $x, 1/2-y, z$.

3.2. Template-exchange reaction of $[V_{18}O_{42}(H_2O)]^{12-}$

The template-exchange reaction of $Na_{12}[V^{IV}{}_{18}O_{42}(H_2O)]\cdot 23H_2O$ with $NaHCO_3$, NaN_3, NaSCN, and $NaNO_3$ led to mixed-valent complexes $Na_6H_4[V^{IV}{}_{11}V^{V}{}_4O_{36}(CO_3)]\cdot 32H_2O$ (**2**), $Na_{10}H[V^{IV}{}_{12}V^{V}{}_6O_{44}(N_3)]\cdot 30H_2O$ (**3**), $Na_{10}H_2[V^{IV}{}_{13}V^{V}{}_5O_{44}(SCN)]\cdot 30H_2O$ (**4**) and $Na_6H_3[V^{IV}{}_{14}V^{V}{}_4O_{42}(NO_3)]\cdot 27H_2O$ (**5**) with yields 77, 32, 22, and 44% based on $Na_{12}[V_{18}O_{42}(H_2O)]\cdot 23H_2O$, respectively. The structures of complexes **2**–**5** have been determined by single crystal X-ray diffraction methods [22]. The bond-valence calculations for **2**–**5** suggested that V^V centers were disordered over the shell framework. The reaction scheme of the template-exchange of $[V_{18}O_{42}(H_2O)]^{12-}$ is shown in Fig. 5 where structure, V^{IV}/V^V ratio, symmetry, and yield for **2**–**5** are represented. The high yield of **2** is due to a high stability of the anion framework of $[V_{15}O_{36}(CO_3)]^{10-}$, which is attributed to the shell framework for the three O atoms of CO_3^{2-} in O(C)···V distances of 2.33(2) Å (mean) with a resultant formation of the contracted $\{V_{15}O_{36}\}$ shell consisting of 3 VO_6 octahedra and 12 VO_5 square pyramids. On the other hand, $\{V_{18}O_{44}\}$ and $\{V_{18}O_{42}\}$ shells for **3**–**5** constructed of linking 18 tetragonal OVO_4 pyramids with weak template ↔ shell interactions: the shortest N···V distances for **3** is 3.140(5) Å, N···V and S···V for **4** 2.766(6) and 3.164(6) Å respectively, and O(N)···V for **5** 2.59(8) Å. The anions for **2** and **3** were mixed-valence isomers for $[V_8^{IV}V_7^{V}O_{36}(CO_3)]^{7-}$ and $[V_{15}^{IV}V_3^{V}O_{44}(N_3)]^{14-}$ (or $[V_8^{IV}V_{10}^{V}O_{44}(N_3)]^{7-}$) respectively, which have been produced photochemically and/or thermochemically [2,3,12,13]. There was no significant difference in IR spectrum and X-ray crystallographic structure between the mixed-valence isomers. As exemplified for the $\{V_{15}O_{36}(CO_3)\}$ cluster, however, it is noted that an increase of the V^{IV}/V^V ratio resulted in a decrease (by 0.1–0.3 Å) of V···V distances, due to modification of the electrostatic repulsion between V atoms. The D_{2h}-$\{V_{18}O_{44}\}$ shell for the $[V_{12}^{IV}V_6^{V}O_{44}(N_3)]^{11-}$ anion produced by the N_3^--exchange reaction of $[V_{18}^{IV}O_{42}(H_2O)]^{12-}$ was the same as by the SCN^--exchange reaction. The D_{2h}-$\{V_{18}O_{44}\}$ shell for the $[V_{13}^{IV}V_5^{V}O_{44}(SCN)]^{12-}$ anion of **4** is different from the D_{2d}-$\{V_{22}O_{54}\}$ shell for $[V_8^{IV}V_{14}^{V}O_{54}(SCN)]^{7-}$, the one prepared by the reaction between $[V_{12}^{IV}V_6^{V}O_{41}(V^{V}O_4)(OH)_9]^{8-}$ and SCN^- at 75°C [16]. The D_{2d}-$\{V_{22}O_{54}\}$ shell is also discussed in the above section for the MoO_4^{2-}-encapsulated complex **1**. The SCN^- ion in both shells $\{V_{18}O_{44}\}$ and $\{V_{22}O_{54}\}$ is disordered. The result

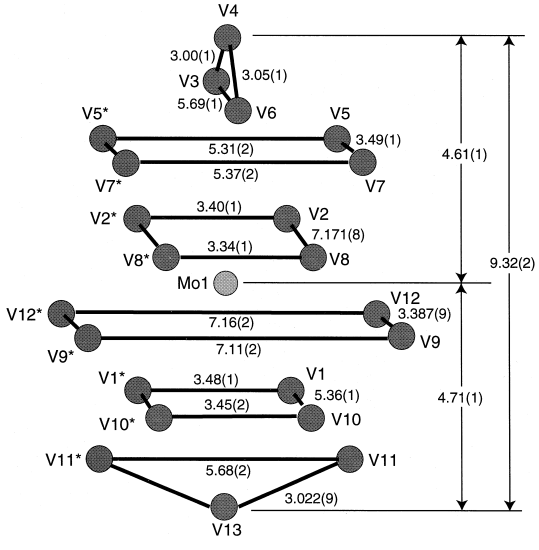

Fig. 4. Vanadium framework for $[V_{12}O_{54}(MoO_4)]^{8-}$. Asterisked atoms are related to corresponding unasterisked ones by a symmetry equivalent ($x, 1/2-y, z$).

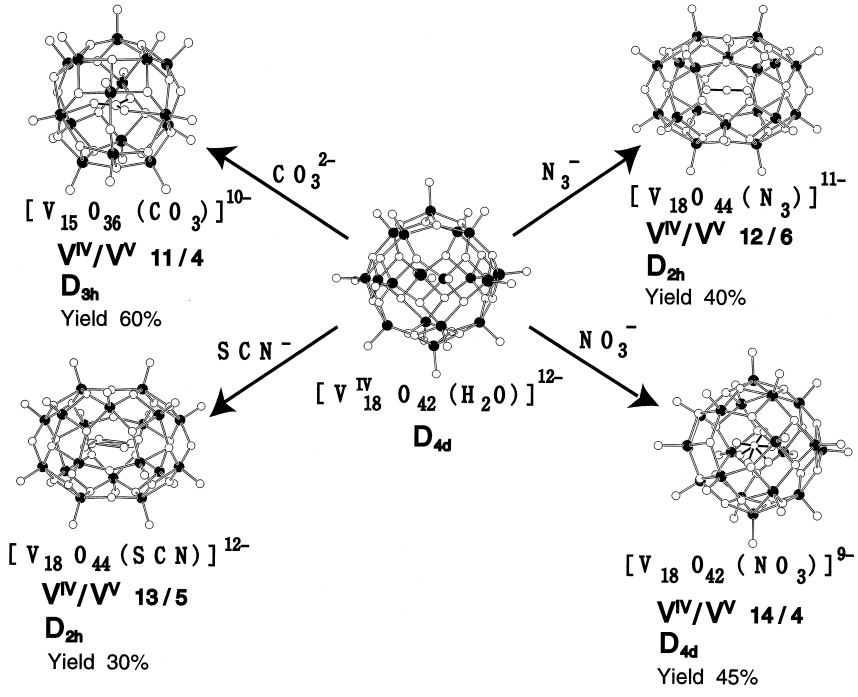

Fig. 5. Schematic representation of the structures for the template-exchange reaction of $[V_{18}O_{42}(H_2O)]^{12-}$. V^{IV}/V^V ratio, symmetry, and yield of **2**–**5** are depicted in figure. Central templates SCN^- and NO_3^- for **4** and **5** are disordered.

of the SCN^--encapsulated shell reveals that the highly symmetric SCN^- template (with $D_{\infty h}$ symmetry) provides an alternative shell of D_{2h}-$\{V_{18}O_{44}\}$ or D_{2d}–$\{V_{22}O_{54}\}$ as a subgroup of $D_{\infty h}$, what reflects an extent of disordered of the template. The NO_3^--encapsulated $[V^{IV}_{14}V^{V}_{4}O_{42}(NO_3)]^{9-}$ anion for **5** consists of the disorder NO_3^- anion and the D_{4d}-$\{V_{18}O_{42}\}$ shell, indicating that the template exchange occurs without geometric change in the shell of the starting anion $[V^{IV}_{18}O_{42}(H_2O)]^{12-}$. It is interesting that the NO_3^--template did not provide the D_{3h}-$\{V_{15}O_{36}\}$ shell observed for the CO_3^{2-}-encapsulation, since the similarity in both size and symmetry (D_{3h}) between NO_3^- and CO_3^{2-} let us conceive the formation of the same shell. The difference in the geometry of the shell between the two templates can be explained in terms of charge and disorder of the template. With the more charged anion of CO_3^{2-} the interaction with the V centers in the shell is increased and the separation (2.29(2)–2.35(1) Å) becomes less, resulting in a preferential formation of the more contracted D_{3h}-$\{V_{15}O_{36}\}$ shell. On the other hand, the NO_3^- template appears to occupy a spherical site where D_{3h} symmetry no longer holds due to disordering. This enables the shell to take D_{4d}-$\{V_{18}O_{42}\}$. The D_{4d}-$\{V_{18}O_{42}\}$ shell for $[V^{IV}_{14}V^{V}_{4}O_{42}(NO_3)]^{9-}$ is also different from the C_2–$\{V_{18}O_{44}\}$ shell for $[V^{IV}_{12}V^{V}_{6}O_{44}(NO_3)]^{11-}$ which was produced in the $KVO_3/N_2H_5OH/HNO_3$ system at 90°C and therein NO_3^- (with the shortest O(N) · · · V > 2.78 Å) is not disordered [16]. Since the symmetry of C_2 of the latter shell is a subgroup of D_{3h}, the formation of the NO_3^--encapsulated D_{4d}-$\{V_{18}O_{42}\}$ shell for $[V^{IV}_{14}V^{V}_{4}O_{42}(NO_3)]^{9-}$ indicates that the disorder of the template is an important factor for the construction of the shell framework. Thus, the disordered NO_3^- anion in the $V_{18}O_{42}$ shell cavity let the shell retain the most spherical shell of D_{4d}-$\{V_{18}O_{42}\}$ without a conformation change to D_{3h}-$\{V_{15}O_{36}\}$ or C_2-$\{V_{18}O_{44}\}$ shell.

As shown in Fig. 5, it should be recalled that the template-exchange of $[V^{IV}_{18}O_{42}(H_2O)]^{12-}$ re-

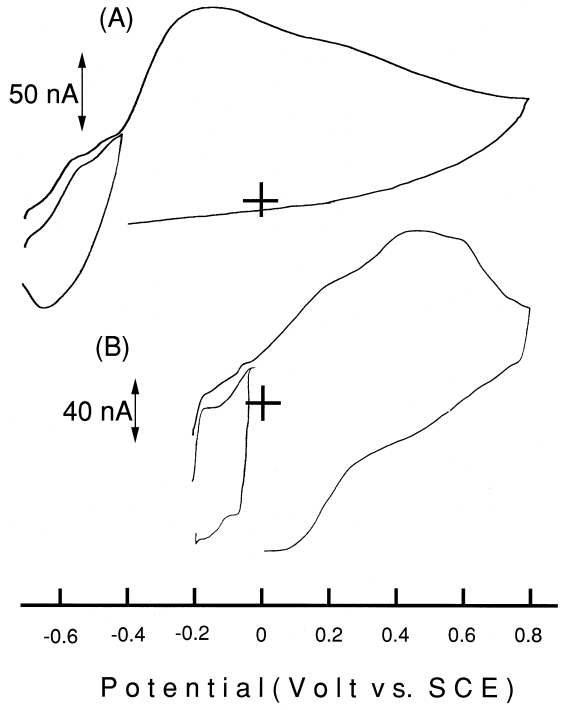

Fig. 6. Cyclic voltammograms observed in aqueous medium containing 5 mM $Na_{12}[V_{18}O_{42}(H_2O)]\cdot 23H_2O$ and 50 mM NaOH (curve *A*), and 0.8 mM $Na_{10}H[V_{18}O_{44}(N_3)]\cdot 30H_2O$ (**3**) and 0.1 M NaCl (curve *B*); scan rate: 1.0 and 1.4 mV/s for *A* and *B* curves, respectively.

sults in the partial oxidation of $OV^{IV}O_4$ sites in the shell. The deaeration of the solution containing $[V^{IV}_{18}O_{42}(H_2O)]^{12-}$ led to low yields of template-exchanged products for N_3^- and NO_3^- (17 and 26% based on $Na_{12}[V_{18}O_{42}(H_2O)]\cdot 23H_2O$, respectively), if other parameters (of concentration, reaction time, and temperature) were not varied. The cyclic voltammetry of $[V^{IV}_{18}O_{42}(H_2O)]^{12-}$ in aqueous solutions (at pH 14) showing a rest potential at -0.70 V showed oxidation ($V^{IV}\rightarrow V^{V}$) peaks at -0.55, -0.44, -0.16, and 0.30 V (vs. SCE), as shown in Fig. 6. The first two waves accompany a composite reduction peak around -0.62 V, implying the pseudo-reversible one-electron redox processes in the $[V^{IV}_{18}O_{42}(H_2O)]^{12-}$ framework. The other peaks were irreversible and broad due to multi-electron oxidations. The cyclic voltammetry of the mixed-valence complexes for the CO_3^{2-}-, N_3^--, SCN^--, and NO_3^--encapsulated $\{V_{15}O_{36}\}$, $\{V_{18}O_{44}\}$, and $\{V_{18}O_{42}\}$ shells for **2**–**5** showed similar multi-electron processes, including several pseudo-reversible sets. Fig. 6 also exemplifies the cyclic voltammetry of $[V^{IV}_{12}V^{V}_{6}O_{44}(N_3)]^{11-}$ for **3** in aqueous solutions which shows the rest potential at -0.21 V and three pseudo-reversible oxidation (at -0.14, -0.10, and 0.20 V) and reduction (at -0.17, -0.04, and 0.10 V) peaks. $[V^{IV}_{14}V^{V}_{4}O_{42}(NO_3)]^{9-}$ was transformed to $[V^{IV}_{12}V^{V}_{6}O_{44}(N_3)]^{11-}$ within 4 days at room temperature after mixing (at pH 8.7) of the aqueous solution (20 ml) of NaN_3 (4 g) into the aqueous solution (30 ml) of **4** (0.1 g), whereas the conversion from $[V^{IV}_{8}V^{V}_{7}O_{36}(CO_3)]^{7-}$ to $[V^{IV}_{14}V^{V}_{4}O_{42}(NO_3)]^{9-}$ hardly proceeded. The fact that the template-exchange results from the oxidation of the shell indicates that the template-exchange reaction occurs via oxidative splitting of a V^{IV}–O–V^{IV} bond of the $\{V_{18}O_{42}\}$ shell by oxygen molecule, to allow one template to exit the cage and another to enter with an involvement of their coordination to the V^{V} atom leading to formation of the V^{IV}/V^{V} mixed-valence cluster shell.

Acknowledgements

We acknowledge Grants-in-Aid for Scientific Research, Number 09218220, Number 09354009, and Number 10304055 for the Ministry of Education, Science, Sports, and Culture for support of this work.

References

[1] T. Yamase, R. Watanabe, Inorg. Chim. Acta. 77 (1983) L193.
[2] T. Yamase, K. Ohtaka, J. Chem. Soc. Dalton Trans., 1994, 2599, Part 1.
[3] T. Yamase, K. Ohtaka, M. Suzuki, J. Chem. Soc. Dalton Trans., 1996, 283, Part 2.
[4] T. Yamase, M. Suzuki, K. Ohtaka, J. Chem. Soc. Dalton Trans., 1997, 2463, Part 3.
[5] T. Yamase, Chem. Rev. 98 (1998) 307.
[6] J. Fischer, L. Ricard, R. Weiss, J. Am. Chem. Soc. 98 (1976) 3050.

[7] F. Robert, M. Leyrie, G. Hervé, A. Tézé, Y. Jeannin, Inorg. Chem. 19 (1980) 1746.
[8] T.L. Jorris, M. Kozik, L.C. Baker, Inorg. Chem. 29 (1990) 1746.
[9] M.H. Alizadeh, S.P. Harmalker, Y. Jeannin, J. Martin-Frere, M.T. Pope, J. Am Chem. Soc. 107 (1985) 2662.
[10] J.T. Rijssenbeek, D.J. Rose, R.C. Haushalter, J. Zubieta, Angew. Chem. Int. Ed. Engl. 36 (1997) 1008.
[11] C.J. Warren, D.J. Rose, R.C. Haushalter, J. Zubieta, Inorg. Chem. 37 (1998) 1140.
[12] M.T. Pope, A. Müller, Angew. Chem. Int. Ed. Engl. 30 (1991) 34, and refs. therein.
[13] A. Müller, H. Reuter, S. Dillinger, Angew. Chem. Int. Ed. Engl. 34 (1995) 2328, and refs. therein.
[14] A. Müller, F. Peters, M.T. Pope, D. Gatteschi, Chem. Rev. 98 (1998) 239, and refs. therein.
[15] A. Müller, E. Krickemeyer, M. Penk, R. Rohlfing, A. Armatage, H. Bögge, Angew. Chem. Int. Ed. Engl. 30 (1991) 1674.
[16] A. Müller, R. Rohlfing, E. Krickemeyer, H. Bögge, Angew. Chem. Int. Ed. Engl. 32 (1993) 909.
[17] P. Román, A. San José, A. Luque, J.M. Gutiérrez-Zorrilla, Inorg. Chem. 32 (1993) 775.
[18] G.K. Johnson, E.O. Schlemper, J. Am. Chem. Soc. 100 (1978) 3645.
[19] G.J. Gilmore, J. Appl. Crystallogr. 42 (1984) 46.
[20] Molecular structure, TEXSAN Single-crystal Sructure Analysis Software, MSC, 3200A Research Forest Drive, The Woodlands, TX 77381, USA, 1989.
[21] I.D. Brown, K.K. Wu, Acta Crystallogr., Sect. B 32 (1976) 1957.
[22] T. Yamase, K. Fukaya, L. Yang, paper in preparation.